Polymer Chemistry

Accepted Manuscript

ROYAL SOCIETY OF CHEMISTRY

www.rsc.org/polymers

Journal Name

ARTICLE

Fabrication of porous organic polymers in the form of powder, soluble in organic solvents and nanoparticles: a unique platform for gas adsorption and efficient chemosensing

Received 00th January 20xx,
Accepted 00th January 20xx

DOI: 10.1039/x0xx00000x

www.rsc.org/

Sujoy Bandyopadhyay, Pragyan Pallavi, Amith G. Anil and Abhijit Patra*

Conjugated porous organic polymers based on novel core of tetraphenyl-5,5-dioctylcyclopentadiene (TPDC) have been fabricated in the form of powder (P1), soluble in common organic solvents (P2) as well as aqueous dispersion of nanoparticles (P3). Fine tuning of the conditions of polycondensation reactions involving tetrakis(4-bromophenyl)-5,5-dioctylcyclopentadiene and diethynyl benzene leads to the formation of TPDC based polymers in three different forms. P1, P2 and P3 possess high thermal stability (up to 375°C) and are porous in nature. Brunauer-Emmett-Teller (BET) surface area and total pore volume of P1 were estimated to be 405 m^2g^{-1} and 0.68 cm^3g^{-1} respectively. Solid P1 was explored for hydrogen and carbon dioxide adsorption. Solution of P2 and aqueous dispersion of P3 exhibit strong cyan fluorescence and are applied for the sensing of nitroaromatics. Steady state and time resolved fluorescence measurements reveal the underlying photophysics of amplified fluorescence quenching of P2 and P3 by nitroaromatics. Porosity, gas adsorption, as well as solubility, strong fluorescence and sensing capabilities establish TPDC based porous polymers as new multifunctional materials and can find broad applications in sensing and optical devices.

Introduction

Porous organic polymers (POPs) have become an appealing field of research owing to their promising applications in various technological fields.[1] POPs with high surface areas have been used mostly in gas storage, separation and heterogeneous catalysis.[2-4] Of late, combination of porosity and π-conjugation leads to the development of the field of conjugated microporous organic polymers (CMPs).[5-10] Such π-conjugated porous materials possess immense potential in various optoelectronic and biological applications ranging from energy storage,[7] tunable emission and light harvesting,[8] to chemo and biosensors.[9] Recently mechanistic details on the origin of microporosity through the network forming Sonogashira cross coupling reactions has been demonstrated.[10] Computational methodologies have also been developed to understand the network structure in POPs as well as to predict the novel design principles.[11]

In spite of having interesting properties, poor solubility and hence difficulty in processability of POPs has posed a major bottleneck for their device integration and practical applications.[12] Attempts were made to achieve desired solubility by fine tuning the structure and rigidity of macromolecular building blocks.[13] Maintaining microporous structure and π-conjugation, pyrene based soluble hyperbranched polymers and linear polymers have been synthesized.[14] Preparation of solution dispersible POP nanoparticles is found to be another approach that has gained significant attention.[15] However, the challenge remains to develop new multifunctional materials integrating the different

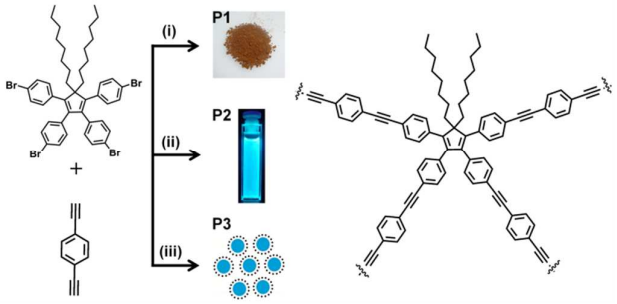

Scheme 1 Fabrication of porous organic polymers involving TBDC (tetrakis-(4-bromophenyl)-5,5-dioctylcyclopentadiene) and DEB (diethynyl benzene) in the form of powder (**P1**), soluble in organic solvents (**P2**) and aqueous dispersion of nanoparticles (**P3**). Fabrication conditions: (i) [$Pd(PPh_3)_4$], CuI, diisopropylamine, toluene, 80°C, 48 h, (ii) [$Pd(PPh_3)_2Cl_2$], CuI, diisopropylamine, toluene, 80°C, 12 h and (iii) [$Pd(PPh_3)_4$], CuI, SDS, water, diisopropylamine, toluene, 50°C, 48 h.

Department of Chemistry, Indian Institute of Science, Education and Research (IISER) Bhopal, Bhopal-462066, Fax: +91 (0)755 409 2392; Tel: +91 (0)755 669 2378;
E-mail: abhijit@iiserb.ac.in
† Electronic Supplementary Information (ESI) available: [details of synthesis and characterizations, fabrication of nanoparticles, microscopy, surface area analysis, computational and spectroscopic investigations and sensing studies]. See DOI: 10.1039/x0xx00000x

properties like microporosity, gas adsorption in one hand and solubility, processability as well as strong fluorescence and sensing capabilities on the other hand. Fine tuning of covalent and non-covalent interactions and polymerization conditions can hold the key for the realization of the above mentioned theme.

Addressing the issue, herein we have developed soluble, conjugated and strongly fluorescent POPs employing a novel core of tetraphenyl-5,5-dioctylcyclopentadiene (TPDC). Fine tuning of the polymerization reactions involving tetrakis(4-bromophenyl)-5,5-dioctylcyclopentadiene (TBDC) and diethynyl benzene (DEB) as monomers allow us to obtain TPDC based POPs (Scheme 1) in the form of insoluble powder (P1), soluble in common organic solvents (P2) as well as aqueous dispersion of nanoparticles (P3). Surface area analysis coupled with molecular dynamics simulations, microscopic, steady state and time resolved spectroscopic investigations provide a unified picture of network structure, physicochemical properties and efficient sensing capabilities of TPDC based POPs. Fabrication of cyclopentadiene based POPs in three different forms, solid, solution and nanoparticles starting from the same monomer and comonomer and exploration of their gas adsorption and sensing potential, to the best of our knowledge, have not been reported in the context of porous organic materials.

Results and discussion

TBDC was prepared from tetraphenyl cyclopentadienone. Alkyl chains in TBDC impart flexibility in the resultant network. Fine tuning of concentration of catalyst, time and temperature of (A_4 + B_2) type Sonogashira cross-coupling polycondensation led to the formation of P1, P2 and P3 (Scheme 1). Soluble polymer and nanoparticles were precipitated by adding toluene solution of P2 and water dispersion of P3 into excess of cold methanol respectively. The precipitated polymers were thoroughly washed by multiple Soxhlet extractions with different solvents. Finally, P2 and P3 obtained in the form of powders are soluble in common organic solvents like tetrahydrofuran, dichloromethane, chloroform, toluene and dimethyl formamide.

The FTIR spectra of TPDC POPs (P1, P2, P3) show characteristic band at 2200 cm^{-1} corresponding to C≡C stretching indicating coupling between TBDC and DEB (Fig. S1-S3). The signal at 89 ppm in ^{13}C NMR spectrum of P2 and P3 further confirms the presence of C≡C (Fig. S6). Thermogravimetric analysis (TGA) showed that all the polymers P1, P2 and P3 are thermally stable up to 375°C (Fig. S7). The weight average molecular weight (M_w) of P2 was found to be 16 kDa with polydispersity index 1.2, as measured by gel permeation chromatography (GPC). Field-emission scanning electron microscopy (FESEM) showed plate like morphology for P1 (Fig. 1a). Rapidly precipitated powder of P2 was found to exhibit aggregated sphere like morphology with average diameter less than 100 nm (Fig. 1b). Aqueous dispersion of P3 revealed nanoparticles with spherical

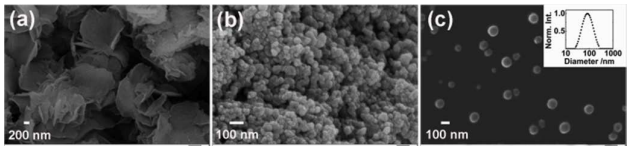

Fig. 1 FESEM images of (a) **P1**, (b) **P2** and (c) **P3**; inset: DLS profile of aqueous dispersion of **P3**.

morphology (Fig. 1c). Average diameter of the particles ranges from 70-110 nm, as estimated by FESEM and corroborated with the profile obtained by dynamic light scattering (DLS) measurements (Fig. 1c, inset).

Nitrogen sorption profile of P1 at 77 K indicates type II isotherm (Fig. 2a). Gas uptake at low relative pressures (P/P_0 < 0.1) signifies microporous character. A large hysteresis loop observed at relative pressure P/P_0 = 0.5 indicates existence of mesopores, originating probably due to interparticulate voids.[7,14] The Brunauer-Emmett-Teller (BET) surface area and total pore volume of P1 were estimated to be 405 m^2g^{-1} and 0.68 cm^3g^{-1} respectively. Pore size distribution (Fig. 2a, inset) calculated by nonlocal density function theory (NLDFT) method revealed that the micropores are centered at 1.4 nm, whereas mesopores range from 3 to 15 nm. Hydrogen and carbon dioxide uptake of P1 (Fig. 2b) were estimated to be 68 cm^3g^{-1} (3.04 $mmolg^{-1}$ at 1 bar, 77K) and 16 cm^3g^{-1} (0.71 $mmolg^{-1}$ at 1 bar, 298K). The nitrogen adsorption-desorption isotherms of P2 and P3 revealed porous nature with BET surface area 39 m^2g^{-1} and 143 m^2g^{-1} respectively (Fig. S11, Table S2).

In order to gain insight into molecular level structure and to understand the porous nature of TPDC based polymers, an atomistic model was built and molecular dynamics simulations were carried out.[11a] Grand canonical Monte Carlo (GCMC) simulations were performed at 77 K to obtain nitrogen sorption.[11b] The characteristics of the simulated model (Fig. 3) were found to be quite consistent with the experimental observations for P1.† The solvent accessible surface area and pore volume calculated using probe radius of 1.82 Å (the kinetic radius of N_2) was found to be 345 m^2g^{-1} and 0.45 cm^3g^{-1}

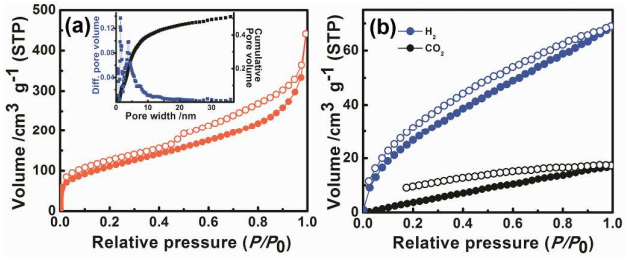

Fig. 2 (a) Nitrogen sorption isotherms (filled circles: adsorption, hollow circles: desorption) of **P1** measured at 77 K. Inset: pore- size distribution profiles estimated using the NLDFT method (blue squares: differential pore volume and black squares: cumulative pore volume). (b) Gas sorption isotherms of **P1** for hydrogen (blue) at 77 K and carbon dioxide (black) at 298 K (filled circles: adsorption, hollow circles: desorption).

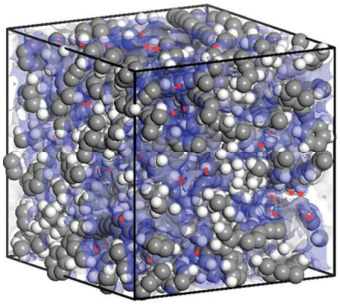

Fig. 3 Snapshot of nitrogen sorption in simulated amorphous cell of TPDC based POPs at 1 bar and 77 K (red dots: density field of adsorbed nitrogen molecules, blue shades: solvent accessible surfaces).

respectively (Fig. S12).

Solid P1 does not show any detectable fluorescence. However, besides porous characters, solution of P2 and aqueous dispersion of P3 were found to be strongly fluorescent. Electronic absorption and emission spectra of P2 in tetrahydrofuran (THF) show absorption with λ_{max} at 365 nm and strong fluorescence (Φ_f = 27%) with λ_{max} at 468 nm (Fig. 4a). Aqueous dispersion of P3 exhibits absorption with λ_{max} at 340 nm and emission (Φ_f = 8%) peaks at 470 nm (Fig. 4b).† The intense absorption band of TPDC POPs is assignable to the π–π* transition of the conjugated framework. Absorption and emission maxima of polymers (P2 and P3) were found to be red shifted compared to that of the TPDC core showing λ_{max}^{abs} at 326 nm and λ_{max}^{em} at 427 nm (Fig. S15). The observed red shift can be attributed to the three dimensional extended π-conjugated framework in polymers.[9a] The fluorescence excitation spectra of P2 and P3 (Fig. 4) are found to be very similar to the absorption spectra indicating that the emission is initiated by a vertical excitation process. The excited state dynamics were investigated using time-correlated single-photon counting experiment. The weighted average lifetimes of P2 in THF and aqueous dispersion of P3 are found to be 0.94 and 0.68 ns respectively (Fig. S17, Table S3).

Strong fluorescence and porosity in P2 and P3 prompted us to explore their potential in chemosensing. A range of electron deficient nitroaromatic compounds (NC) like nitrobenzene,

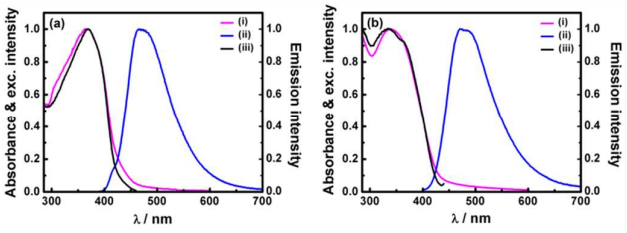

Fig. 4. (a) Spectroscopic features of **P2** in THF: normalized (i) absorption (ii) emission (λ_{exc} = 365 nm) and (iii) excitation (λ_{em} = 468 nm) spectra. (b) Spectroscopic features of aqueous dispersion of **P3**: normalized (i) absorption (ii) emission (λ_{exc} = 340 nm) and (iii) excitation (λ_{em} = 470 nm) spectra.

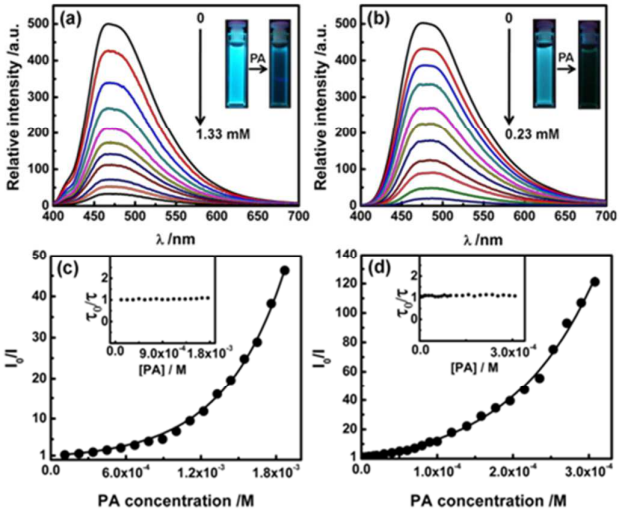

Fig. 5 (a) Emission spectra demonstrating the quenching of fluorescence of (a) **P2** in THF (λ_{ex} = 365 nm) and (b) **P3** in water (λ_{ex} = 340 nm) with increasing concentrations of picric acid (PA). Inset: photographs of (a) **P2** (b) **P3** before and after addition of PA under the illumination of UV light at 365 nm. Stern-Volmer plots of I_0/I against concentration of PA (I_0 = fluorescence intensity at [PA] = 0 M) of (c) **P2** in THF and (d) **P3** in water; the inset graphs refer to plots of corresponding relative fluorescence lifetime (τ_o/τ) against various concentrations of PA (τ_o = lifetime of polymer in absence of PA).

m-dinitrobenzene, 2,4-dinitrotoluene and picric acid (PA) was chosen as electron deficient analytes. Upon successive addition of NC, fluorescence intensity of THF solution of P2 and aqueous dispersion of P3 decreases gradually (Fig. 5a, b and Fig. S19a-S24a). PA being most electron deficient exhibits best quenching efficiency. At a PA concentrations of 1.33 and 0.23 mM fluorescence signals of P2 and P3 were quenched by 93% and 98% respectively (Fig. 5a and b, inset). Further addition of PA led to complete quenching. Quenching of fluorescence of P3 can be observed at a PA concentration as low as 2 ppm indicating high sensitivity. The Stern-Volmer plots bend upwards for P2 and P3 on increasing concentration of NC suggesting an amplified quenching (Fig. 5c, d and Fig. S19b-S24b).[16] No significant decrease of average fluorescence lifetimes of P2 and P3 with increasing concentrations of NC indicates that the quenching process is likely to be static in nature (Fig. 5c and d, inset).[17]† Such amplified static quenching can be attributed to the loose ground state association of nitroaromatic molecules into the pores of P2 and P3.[18] Accordingly, quenching sphere model was employed to fit the quenching data (Fig. 5c, d and Fig. S19b-S24b); the static quenching constants for P2 and P3 at lower concentrations of PA were found to be 2.1 × 10^3 and 7.6 × 10^4 L mol^{-1} respectively.[17,18]† The quenching efficiency of nitroaromatic compounds towards P2 and P3 was found to follow the order NB < DNB < DNT < PA, consistent with the trend reported earlier for other covalent organic polymers (Table S6 and S7).[19] As indicated, nanoparticle dispersions (P3) exhibit enhanced quenching compared to that of isolated species in THF (P2). It

is presumably due to the higher surface area and more accessible cavities leading to efficient interactions of nitroaromatic molecules with the nanoaggregates.[16,18]

Conclusions

A convenient protocol has been demonstrated to fabricate cyclopentadiene based porous organic polymers in three different forms: powder (P1), soluble in organic solvents (P2) and aqueous dispersion of nanoparticles (P3). Solid P1 was explored for hydrogen and carbon dioxide adsorption while soluble counterparts P2 and P3 demonstrate efficient sensing of picric acid by amplified fluorescence quenching. Currently, we are exploring the possibility of fluorescence tuning by attaching suitable acceptor dyes at the surface of nanoparticles. Preliminary exploration suggests facile energy transfer from nanoparticles P3 to surface-bound Rhodamine 6G molecules leading to switching of emission towards longer wavelength regions (Fig. S26). The current study paves the way for the development of multifunctional materials based on porous organic polymers.

Experimental

General methods

All reagents and solvents were purchased from commercial sources and used without purification. ^{1}H and ^{13}C-NMR spectra were recorded on Bruker Avance III 500, 700 MHz NMR spectrometers. FTIR measurements were carried out on Perkin Elmer FTIR spectrophotometer. Thermogravimetric analysis (TGA) was carried out using Perkin Elmer TGA-6000 instrument. The samples were heated at a rate of 10^{o}C min^{-1} under a nitrogen atmosphere to a maximum of 900^{o}C. Molecular weights of the soluble polymers were estimated by Gel Permeation Chromatography (GPC, Polymer Laboratories). THF was used as the eluent with flow rate of 1 mL/min at 40°C and polystyrene was used as the calibration standard. Universal calibration was used employing refractive index and viscometry detectors. Ultrasonication was carried out with Branson sonifier (model: W-450) using microtip of 5 mm tip diameter.

The surface morphology of all polymers and size of the nanoparticles were examined using Carl Zeiss (Ultraplus) field emission scanning electron microscope (FESEM). Energy dispersive X-ray spectroscopy was examined using a spectrometer (Oxford Instruments X-Max^{N}) attached to FESEM. Dynamic light scattering (DLS) measurements of aqueous dispersion of nanoparticles (P3) were carried out with Beckman Coulter Delso Nano C DLS set up.

All gas adsorption experiments were performed on a Quantachrome Autosorb QUA211011 equipment. Nitrogen adsorption isotherms were analyzed using ASIQwin software. Samples were degassed at 80^{o}C for 12 h under vacuum before analysis. Nitrogen and hydrogen adsorption-desorption isotherms were measured at 77 K and for carbon dioxide at 298 K. Polymer surface area and pore size distributions were measured by nitrogen adsorption-desorption isotherms. The total pore volume of P1 was estimated to be 0.68 cm^{3}g^{-1} according to single point adsorption at P/P_0 = 0.99. Pore size distributions were derived from nonlocal density functional theory (NLDFT) method. Micropore surface area of P1 calculated from the N_2 adsorption isotherm using the t-plot method based on the Halsey thickness equation were found to be 75 m^{2}g^{-1}.

Molecular model of TPDC based polymers was built using Materials Studio 6.1 package (*accelrys).* The model structure of polymer was constructed with net molar mass of 16358 g/mol. All molecular dynamics and energy minimization were performed with Discover module using COMPASS forcefield. Multiple compression and decompression were carried out to equilibrate the amorphous cell.[20] The Noose Hover thermostat during NVT steps and Andersen barostat were used at NPT steps. The final density of relaxed structure was 0.85 g/cm^3. The adsorption isotherm of nitrogen was simulated at 77 K up to 1 bar using GCMC simulation.†

UV-vis absorption spectra were recorded on a Cary 100 spectrophotometer. Steady state fluorescence measurements were carried out on a Jobin Yvon Horiba Model Fluorolog-3-21. The fluorescence quantum yield of P2 in THF and P3 in water were estimated by comparison with coumarin-102 in ethanol (Φ_f = 0.76) and corrected for the refractive index of the solvent.[21] Time-resolved fluorescence measurements were carried out using time-correlated single-photon counting (TCSPC) spectrometer (Delta Flex-01-DD/HORIBA). Delta diode laser 370 nm with FWHM = 154 ps was used as excitation source. Picosecond photon detection module with photomultiplier tube was used as detector. Instrument response function was recorded by using aqueous solution of Ludox. Decay curves were analyzed by nonlinear least-squares iteration using IBH DAS6 (version 6.8) decay analysis software.

Synthesis of monomers:

(i) Tetraphenylcyclopentadiene (TPCP):

Tetraphenylcyclopentadiene (TPCP) was synthesized starting from tetraphenylcyclopentadienone following a reported procedure with minor modifications.[22]

^{1}H NMR: δ_H (500 MHz, $CDCl_3$) 7.22 – 7.11 (16 H, m), 7.00 – 6.96 (4 H, m), 4.04 (2 H, s); ^{13}C NMR: δ_C (126 MHz, $CDCl_3$) 144.55, 139.75, 136.60, 136.48, 129.85, 128.15, 128.05, 127.84, 126.69, 126.40, 45.81; MS (MALDI-TOF): calculated for $C_{29}H_{22}$, 370.48; found 370.19.

(ii) Tetraphenyl-5,5-dioctylcyclopentadiene (TPDC):

TPCP (1g, 2.69 mmol) and tetra-n-butylammonium bromide (262 mg, 0.81 mmol) were dissolved in 5 mL DMSO. 1-Bromo octane (1 mL, 5.92 mmol) and 1.2 mL 50% aqueous NaOH were added to it. The reaction mixture was stirred at 80-90^{o}C for 2 h. After cooling down to room temperature, the reaction mixture was poured into 100 mL of water then extracted three times with chloroform. The organic layer was washed with water and brine solution, dried over $MgSO_4$. After evaporation of the solvent the resulted residue was purified via column chromatography (SiO_2, hexane) and colorless oil was obtained. The liquid was dissolved in ethanol and recrystallized to obtain the pure compound as a colorless solid (0.803 g, 50% yield).

^{1}H NMR: δ_H (500 MHz, $CDCl_3$) 7.21 (4 H, t, *J* 7.5), 7.17 (2 H, d, *J* 7.1), 7.07 (4 H, d, *J* 7.8), 7.06 – 7.01 (6 H, m), 6.82 (4 H, d,

J 7.4), 1.73 – 1.71 (4 H, m), 1.32 – 1.04 (24 H, m), 0.85 (6 H, t, *J* 7.1); ^{13}C NMR: δ_C (126 MHz, $CDCl_3$) 147.75, 144.06, 137.14, 136.17, 130.31, 129.71, 127.93, 127.36, 126.37, 126.06, 64.57, 35.48, 31.84, 29.77, 29.38, 29.23, 23.17, 22.66, 14.12; MS (MALDI –TOF): calculated for $C_{45}H_{54}$, 594.91; found 594.37.

(iii) Tetrakis(4-bromophenyl)-5,5-dioctylcyclopentadiene (TBDC):

TPDC (350 mg, 0.59 mmol) was dissolved in 5 mL $CHCl_3$, then bromine (0.36 mL, 7.05 mmol) was added to it. The reaction mixture was stirred at room temperature for 10 h under protection from light. Then the reaction mixture was poured into 50 mL chloroform and washed three times with sodium thiosulfate solution (1 M) and dried over $MgSO_4$, after evaporating the solvent the residue was purified via column chromatography (SiO_2, hexane) to get a colorless oil. The liquid was dissolved in ethanol and recrystallized to obtain the pure compound as a colorless solid (350 mg, 65% yield).
^{1}H NMR: δ_H (500 MHz, $CDCl_3$) 7.36 (4 H, d, *J* 8.5), 7.20 (4 H, d, *J* 8.5), 6.88 (4 H, d, *J* 8.5), 6.64 (4 H, d, *J* 8.5), 1.69 – 1.66 (4 H, m), 1.26 – 1.04 (24 H, m), 0.86 (6 H, t, *J* 7.1); ^{13}C NMR δ_C (126 MHz, $CDCl_3$) 147.74, 142.95, 135.18, 134.11, 131.72, 131.52, 131.07, 131.06, 121.05, 120.86, 64.80, 35.35, 31.80, 29.62, 29.30, 29.18, 23.16, 22.64, 14.11; MS (MALDI- TOF): calculated for $C_{45}H_{50}Br_4$, 910.49; found 910.04.

Fabrication of polymers in different forms:

(i) Synthesis of polymer in the form of powder (P1):

TBDC (183 mg, 0.2 mmol), 1,4-diethynylbenzene (DEB) (76 mg, 0.6 mmol), copper(I) iodide (1.9 mg, 0.01 mmol) and tetrakis(triphenylphosphine)palladium (23 mg, 0.02 mmol) were dissolved in 10 mL dry toluene and subjected to three times freeze-pump-thaw cycles to remove the dissolved oxygen. Then 10 mL of freshly distilled diisopropylamine was added to it and again the reaction mixture was degassed by three times freeze-pump-thaw cycles. The reaction mixture was stirred for 48 h at 80°C under argon atmosphere and under protection from light. The reaction mixture was brought to room temperature and the precipitate was collected through gravimetric filtration. The precipitate washed with methanol, acetone and chloroform and then rigorously washed by Soxhlet extraction for 24 h each with methanol, acetone, chloroform and ethanol respectively and dried under vacuum at 70°C to give polymer P1 (92 mg, 49% yield:) as a brown solid.
FTIR (ν_{max}/cm^{-1}): 3037, 2926, 2852, 2202, 1596, 1489, 829; EDX analysis (wt%): C 98.74, Br 0.74, Pd 0.53.

(ii) Synthesis of soluble polymer (P2):

TBDC (91 mg, 0.1 mmol), 1,4-diethynylbenzene (DEB, 25 mg, 0.2 mmol), copper(I) iodide (1.3 mg 0.007 mmol), and bis(triphenylphosphine)palladium(II) dichloride (10.5 mg, 0.015 mmol) were dissolved in 20 mL degassed toluene. 20 mL of freshly distilled diisopropylamine was added to it. The reaction mixture was stirred for 12 h at 80°C under argon atmosphere under protection from light. Then the reaction mixture was cooled to room temperature and filtered. The filtrate was precipitated in cold methanol and the precipitate was thoroughly washed with methanol, acetone and then rigorously washed by Soxhlet extraction for 24 h each with methanol and acetone respectively and dried under vacuum at 70°C to give the pure polymer P2 (38 mg, 45% yield) as a yellow solid.
GPC (THF): (M_n = 13 kDa, M_w = 16 kDa) FTIR (ν_{max}/cm^{-1}): 3035, 2925, 2850, 2205, 1595, 1485, 830; ^{1}H NMR: δH (700 MHz; $CDCl_3$) 7.50 – 7.47 (m, Ar-H), 7.43 – 7.31 (m, Ar-H), 7.20 (br, Ar-H), 7.01 (br, Ar-H), 6.90 (b, Ar-H), 6.77 (br, Ar-H), 6.66 (br, Ar-H), 1.71 (m, CH_2), 1.34 – 1.07 (br, CH_2), 0.86 (t, CH_3); EDX analysis (wt%): C 98.51, Br 1.07, Pd 0.42.

(iii) Fabrication of nanoparticles (P3) by miniemulsion polymerization

500 mg of sodium dodecyl sulfate (SDS) was dissolved in 50 mL of degassed water. Dry toluene (1.1 mL) and freshly distilled diisopropylamine (0.7 mL) were added to a mixture of TBDC (91 mg, 0.1 mmol), 1,4-diethynylbenzene (DEB, 38 mg, 0.30 mmol), tetrakis(triphenylphosphine)palladium (8 mg, 0.007 mmol) and copper(I) iodide (0.6 mg, 0.0035 mmol). Then the mixture was added to the surfactant solution while stirring (1200 rpm). After stirring vigorously for 5 min for pre-emulsification, the mixture was ultrasonicated for 2 min under argon flow to obtain a stable miniemulsion. Gentle stirring of the miniemulsion at 50°C under Ar atmosphere for 48 h, formed a stable colloidal dispersion. This dispersion was stirred, open to air for 24 h and filtered over sintered glass crucible.

An aliquot of nanoparticles dispersion was precipitated by addition to excess of cold methanol and collected after washing with water, methanol and acetone, then rigorously washed by Soxhlet extraction for 24 h each with methanol and acetone respectively. Then it was dried under vacuum at 70°C and was used for FTIR and NMR characterizations.
FTIR (ν_{max}/cm^{-1}) 3042, 2928, 2854, 2212, 1592, 1484, 834; ^{1}H NMR: δ_H (700 MHz; $CDCl_3$) 7.50 – 7.47 (m, Ar-H), 7.43 – 7.34 (m, Ar-H), 7.20 (br, Ar-H), 7.01 (br, Ar-H), 6.89 (br, Ar-H), 6.77 (br, Ar-H), 6.70-6.63 (br, Ar-H), 1.71 (m, CH_2), 1.31 – 1.09 (br, CH_2), 0.86 (t, CH_3).

Acknowledgements

Financial support from DST (SB/FT/CS-081/2013), New Delhi and infrastructural support from IISER Bhopal are gratefully acknowledged. SB thanks IISERB and PP thanks UGC for fellowship.

Notes and references

1. (a) J. Germain, J. M. J. Fréchet and F. Svec, *Small*, 2009, **5**, 1098; (b) A. Thomas, *Angew. Chem. Int. Ed.,* 2010, **49**, 8328; (c) R. Dawson, A. I. Cooper and D. J. Adams, *Prog. Polym. Sci.*, 2012, **37**, 530; (d) D. Wu, F. Xu, B. Sun, R. Fu, H. He and K. Matyjaszewski, *Chem. Rev.* 2012, **112**, 3959.
2. (a) T. Ben, H. Ren, S. Ma, D. Cao, J. Lan, X. Jing, W. Wang, J. Xu, F. Deng, J. M. Simmons, S. Qiu and G. Zhu, *Angew. Chem. Int. Ed.,* 2009, **48**, 9457; (b) D. Yuan, W. Lu, D. Zhao and H. C. Zhou, *Adv. Mater.,* 2011, **23**, 3723.

3. (a) E. Preis, C. Widling, U. Scherf, S. Patil, G. Brunklaus, J. Schmidt and A. Thomas, *Polym. Chem*., 2011, **2**, 2186; (b) Q. Chen, M. Luo, P. Hammershøj, D. Zhou, Y. Han, B. W. Laursen, C. G. Yan and B. H. Han, *J. Am. Chem. Soc*., 2012, **134**, 6084; (c) S. Chakraborty, Y. J. Colón, R. Q. Snurr and S. T. Nguyen, *Chem. Sci*., 2015, **6**, 384.
4. (a) Q. Liang, J. Liu, Y. Wei, Z. Zhao and M. J. MacLachlan, *Chem. Commun.,* 2013, **49**, 8928; (b) R. K. Totten, Y. S. Kim, M. H. Weston, O. K. Farha, J. T. Hupp and S. T. Nguyen, *J. Am. Chem. Soc.,* 2013, **135**, 11720.
5. (a) A. I. Cooper, *Adv. Mater*., 2009, **21**, 1291; (b) F. Vilela, K. Zhang and M. Antonietti, *Energy Environ. Sci*., 2012, **5**, 7819; (c) Y. Xu, S. Jin, H. Xu, A. Nagai and D. Jiang, *Chem. Soc. Rev.,* 2013, **42**, 8012.
6. (a) K. V Rao, S. Mohapatra, T. K. Maji and S. J. George, *Chem. Eur. J.,* 2012, **18**, 4505; (b) K. Zhang, D. Kopetzki, P. H. Seeberger, M. Antonietti and F. Vilela, *Angew. Chem. Int. Ed*., 2013, **52**, 1432; (c) Y. Xie, T. T. Wang, X. H. Liu, K. Zou and W. Q. Deng, *Nat. Commun*., 2013, **4**, DOI: 10.1038/ncomms2960; (d) H. Bildirir, J. P. Paraknowitsch and A. Thomas, *Chem. Eur. J*. 2014, **20**, 9543; (e) Y. Liao, J. Weber and C. F. J. Faul, *Chem. Commun.,* 2014, **50**, 8002.
7. F. Xu, X. Chen, Z. Tang, D. Wu, R. Fu and D. Jiang, *Chem. Commun*., 2014, **50**, 4788.
8. L. Chen, Y. Honsho, S. Seki and D. Jiang, *J. Am. Chem. Soc*., 2010, **132**, 6742.
9. (a) Y. Zhang, S. A, Y. Zou, X. Luo, Z. Li, H. Xia, X. Liu and Y. Mu, *J. Mater. Chem. A*, 2014, **2**, 13422; (b) C. Gu, N. Huang, J. Gao, F. Xu, Y. Xu and D. Jiang, *Angew. Chem. Int. Ed*., 2014, **53**, 4850.
10. A. Laybourn, R. Dawson, R. Clowes, T. Hasell, A. I. Cooper, Y. Z. Khimyak and D. J. Adams, *Polym. Chem*., 2014, 5, 6325.
11. (a) J. X. Jiang, F. Su, A. Trewin, C. D. Wood, H. Niu, J. T. A. Jones, Y. Z. Khimyak and A. I. Cooper, *J. Am. Chem. Soc*. 2008, **130**, 7710; (b) L. J. Abbott and C. M. Colina, *Macromolecules*, 2011, **44**, 4511.
12. A. Patra and U. Scherf, *Chem. Eur. J.* 2012, **18**, 10074.
13. (a) N. B. McKeown and P. M. Budd, *Chem. Soc. Rev.*, 2006, **35**, 675; (b) N. B. McKeown and P. M. Budd, *Macromolecules*, 2010, **43**, 5163.
14. (a) G. Cheng, T. Hasell, A. Trewin, D. J. Adams and A. I. Cooper *Angew. Chem. Int. Ed.,* 2012, **51**, 12727; (b) G. Cheng , B. Bonillo, R. S. Sprick , D. J. Adams, T. Hasell and A. I. Cooper, *Adv. Funct. Mater.,* 2014, **24**, 5219.
15. (a) A. Patra, J. M. Koenen and U. Scherf, *Chem. Commun.,* 2011, **47**, 9612; (b) M. G. Schwab, D. Crespy, X. Feng, K. Landfester, K. Müllen., *Macromol. Rapid Commun*., 2011, **32**, 1798; (c) K. Wu, J. Guo and C. Wang, *Chem. Commun*., 2014, **50**, 695; (d) X. Wu, H. Li, Y. Xu, B. Xu, H. Tong and L. Wang, *Nanoscale,* 2014, **6**, 2375.
16. (a) C. Y. K. Chan, Z. Zhao, J. W. Y. Lam, J. Liu, S. Chen, P. Lu, F. Mahtab, X. Chen, H. H. Y. Sung, H. S. Kwok, Y. Ma, I. D. Williams, K. S. Wong and B. Z. Tang, *Adv. Funct. Mater.*, 2012, **22**, 378; (b) W. Dong, T. Fei, A. Palma-Cando and U. Scherf, *Polym. Chem.*, 2014, **5**, 4048.
17. J. R. Lakowicz, *Principles of Fluorescence Spectroscopy*, Springer, New York, 2006.
18. Y. Zhang, G. Chen, Y. Lin, L. Zhao, W. Z. Yuan, P. Lu, C. K. W. Jim, Y. Zhang and B. Z. Tang, *Polym. Chem.*, 2015, **6**, 97.
19. Z. Xiang and D. Cao, *Macromol. Rapid Commun.*, 2012, **33**, 1184.
20. L. J. Abbott, A. G. McDermott, A. D. Regno, R. G. D. Taylor, C. G. Bezzu, K. J. Msayib, N. B. McKeown, F. R. Siperstein, J. Runt and C. M. Colina, *J. Phys. Chem. B*, 2013, **117**, 355.
21. (a) K. Rurak, M. Spieles, *Analytical Chem.,* 2011, **83**, 1232; (b) C. Wurth, M. Grabolle, J. Pauli, M. Spieles, U.R. Genger, *Nature Protocol.,* 2013, **8**, 1535.
22. M. P. Castellani, J. M. Wright, S. J. Geib, A. L. Rheingold, and W. C. Trogler , *Organometallics*, 1986, **5**, 1116.

Graphical Abstract - Table of Content

"Fabrication of porous organic polymers in the form of powder, soluble in organic solvents and nanoparticles: a unique platform for gas adsorption and efficient chemosensing"

by Sujoy Bandyopadhyay, Pragyan Pallavi, Amith G. Anil and Abhijit Patra*

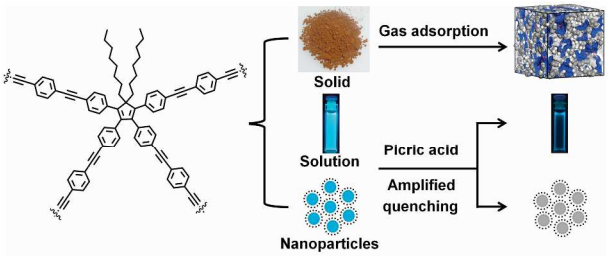

Fabrication of multifunctional porous organic polymers

Tetraphenyl-5,5-dioctylcyclopentadiene based porous organic polymers were fabricated in the form of powder, soluble in organic solvents and nanoparticles and were explored for gas adsorption and chemosensing.